Relational Adequacy and Recursive Boundary Dynamics:

Time as Alignment Cost and Observer-Relative Identity in Boundary-Driven Cellular Automata

Erez Ashkenazi
Yesud Ha'Ma'ala, Upper Galilee 1210500, Israel
erez@noesis-net.org — ORCID: 0009-0001-5461-0459 — https://www.noesis-net.org

Abstract

This paper unifies an ontological equation of state for experienced time with an explicit, falsifiable in-silico testbed for observer-relative identity continuity. *Relational Adequacy* (TRA) treats "experienced time" t not as an external container but as a distortion induced by finitude: when a bounded system attempts to align with an unfolding baseline τ under predictive and coherence constraints. We formalize this as an equation of state,

$$t \;=\; \tau \exp\big(\lambda S_{\text{total}}\big), \qquad S_{\text{total}} = S_{\text{pred}} + \eta S_{\text{coh}}, \tag{1}$$

where S_{pred} is predictive surprisal, S_{coh} is coherence cost, and λ scales misfit into temporal distortion. To test this claim operationally, we construct a boundary-driven cellular automaton (CA) in which boundaries are causal operators: local update thresholds are modulated by a distance-from-boundary field computed from a dynamically defined "skin." Within this dynamics we embed a finite observer subsystem (bounded window, limited memory, optional budgeted intervention) and define identity as continuity of a tracked structure. Empirically, across randomized sweeps under both open (zero) and closed (toroidal) boundary conditions, we obtain a sharp dissociation: memory-coupled tracking (persistence bias) yields high continuity without any intervention, and memory-guided intervention modestly improves continuity under perturbation; however, matched-budget *random* intervention collapses to near-zero continuity despite identical action magnitude. We then specify explicit coherence cost metrics (S_{coh}) from structural discontinuity, memory-halo deviation, and intervention misalignment, enabling direct falsification tests of TRA predictions, including adequacy–identity correlations and exponential misfit-to-identity scaling. The unified framework offers a quantitative bridge from ontology to measurement: experienced time, identity continuity, and viable agency emerge as different faces of the same alignment constraint.

Keywords: relational adequacy; experienced time; alignment cost; temporal distortion; coherence cost; surprisal; boundary-driven cellular automata; observer-relative identity; persistence bias; memory-guided intervention; autopoiesis; enactive cognition; information-thermodynamics.

1 Introduction: The Cost of Being Finite

1.1 One problem, two languages

Physics typically treats time as a coordinate or metric structure; cognition and computation treat time as internal process, workload, or "ticks." These descriptions often remain separate.

This paper proposes a single structural constraint underlying both: *a finite system that persists must continuously align its internal constraints with an unfolding reality.* When this alignment is costly—predictively and coherently—experienced time inflates.

In parallel, classical cellular automata (CA) treat boundaries as emergent descriptors: patterns form, edges appear, and boundaries are drawn after the fact. Biological and cognitive systems invert this: boundaries are *operators* that shape internal dynamics (membranes, interfaces, attentional borders). We adopt the same inversion in a discrete dynamical system: boundaries are explicitly causal in the update rule.

1.2 Core hypothesis

Time, for a finite mode, is the alignment cost of remaining coherent.
Experienced time t scales with total misfit S_{total} relative to a baseline unfolding τ.

1.3 Contributions

This work provides:

1. A TRA equation of state mapping total misfit into experienced time.
2. A boundary-driven CA in which a dynamically defined "skin" modulates local update thresholds via a distance field.
3. An embedded finite observer (bounded window, limited memory, optional budgeted intervention) that operationalizes identity as a maintained tracking relation.
4. A matched-budget random-intervention control showing that *intervention magnitude is insufficient*: informational coupling is necessary.
5. An explicit coherence-cost formalism (S_{coh}) that converts the ontology-to-measurement bridge into a falsifiable quantitative program.

2 Relational Adequacy: An Equation of State for Experienced Time

2.1 Baseline unfolding, distortion, and adequacy

Let τ denote a baseline unfolding parameter (operationally: a reference clock or the CA step index treated as "external baseline"). Let t denote the effective duration experienced or required by a finite mode to remain coherent.

Define temporal distortion and adequacy:

$$D \equiv \frac{t}{\tau}, \qquad\qquad A \equiv \frac{\tau}{t} = \frac{1}{D}. \tag{2}$$

2.2 Total misfit

We decompose total misfit:

$$S_{\text{total}} \equiv S_{\text{pred}} + \eta S_{\text{coh}}, \qquad \eta \geq 0, \tag{3}$$

where S_{pred} is predictive surprisal (negative log-likelihood of observations under a prediction model) and S_{coh} is coherence cost (penalty for discontinuity or constraint-violation relative to memory and organization).

2.3 Equation of state

TRA posits an exponential compression of misfit into adequacy:

$$A = \exp(-\lambda S_{\text{total}}), \qquad \lambda > 0, \tag{4}$$

yielding the equation of state:

$$t = \tau \exp(\lambda S_{\text{total}}). \tag{5}$$

The exponential form is not decorative: it makes a specific, testable functional claim that competes with linear or power-law alternatives (Section 5.3).

3 Recursive Boundary Dynamics in Cellular Systems

3.1 Boundaries as causal operators

Classical CA treat boundaries as either technical conditions (finite-grid edges) or emergent descriptors. Here, boundaries are made causal: local transition thresholds are conditioned on distance from a dynamically computed "skin" boundary. This creates a feedback loop:

$$\text{skin} \to d(x) \to \text{local thresholds} \to \text{new skin}.$$

3.2 Grid, neighborhood, and boundary conditions

We simulate a binary CA on an $H \times W$ grid (default 80×120) with Moore neighborhood and synchronous updates for $T = 300$ steps. Two boundary conditions are tested:

- **Zero mode:** outside-the-grid treated as inactive medium (open world).
- **Wrap mode:** toroidal world (closed control).

3.3 Operational skin and distance-to-boundary coupling

At each step t, the *skin* is defined as active cells adjacent to at least one inactive neighbor. A distance transform gives $D_t(x)$, the distance from each cell x to the nearest skin cell; it is normalized into a boundary-pressure signal $d(x) \in [0, 1]$. Local birth/survival thresholds are modulated by $d(x)$, implementing recursive boundary influence.

3.4 Locality note

The distance transform is a global computation and thus violates strict CA locality by design. This is an explicit modeling choice: we sacrifice strict locality to obtain explicit boundary causality. Future work can approximate $d(x)$ with local diffusion fields to regain locality while preserving boundary causation.

4 Embedded Finite Observer Subsystem

4.1 Attention window and drift

The observer operates within a Chebyshev-radius window of radius r (default $r = 18$). The attention center drifts toward the centroid of the tracked core at bounded speed, modeling limited attentional mobility.

4.2 Core selection and persistence bias

Within the window, connected components of active cells are computed and one component is selected as the tracked *core*:

- **No persistence:** selection is arbitrary (e.g., largest component), independent of prior core.
- **Persistence bias:** selection prefers maximal contact with a *memory halo* (union of dilated past core masks).

A minimum halo-contact threshold implements a discrete "same-thing" criterion.

4.3 Budgeted intervention and matched-budget random control

In active modes, the observer may override cell states within its window up to a per-step budget:

$$B = \lfloor \beta |\text{window}| \rfloor, \qquad \beta = 0.05.$$

We evaluate five modes:

Mode	Memory	Intervention	Target selection
object_off_tracked	no	no	tracking-only baseline
passive_nopersist	no	no	arbitrary
passive_persist	yes	no	memory-guided
active_persist	yes	yes	memory-guided
active_random	no	yes	random (matched budget)

The **active_random** control matches the intervention budget of **active_persist** while eliminating informational coupling.

5 Measurement: Identity Continuity, Misfit, and the TRA Bridge

5.1 Identity score and coherence collapse

Identity is defined operationally as continuity of the tracked core across time. In persistence modes, identity is measured via halo-contact continuity; otherwise, via Jaccard overlap (IoU) between consecutive core masks. An *identity break* is defined by overlap falling below $\theta = 0.05$.

5.2 Explicit misfit computation: S_{coh}, S_{pred}, S_{total}

To avoid inferring coherence directly from the identity metric, we compute explicit per-step misfit within the observer window. Let $C_t \in \{0,1\}^N$ denote the tracked core mask over N window cells, and let H_{t-1} denote the memory halo.

Coherence cost. We compute:

$$S_{\text{coh}}(t) = w_1 S_{\text{struct}}(t) + w_2 S_{\text{mem}}(t) + w_3 S_{\text{int}}(t), \tag{6}$$

with:

$$S_{\text{struct}}(t) \equiv 1 - \text{IoU}(C_t, C_{t-1}), \tag{7}$$

$$S_{\text{mem}}(t) \equiv 1 - \frac{|C_t \cap H_{t-1}|}{|C_t| + \epsilon}, \tag{8}$$

$$S_{\text{int}}(t) \equiv 1 - \frac{|I_t \cap H_{t-1}|}{|I_t| + \epsilon}, \tag{9}$$

where I_t is the intervention mask (active modes). Component-wise reporting and sensitivity analysis over (w_1, w_2, w_3) reduces the risk of weight-tuning artifacts.

Predictive surprisal. Predictive surprisal is defined as cross-entropy under a one-step predicted Bernoulli field $\hat{p}_t(x) \in (0, 1)$:

$$S_{\text{pred}}(t) = -\frac{1}{N} \sum_{x=1}^{N} \Big[C_t(x) \log \hat{p}_t(x) + (1 - C_t(x)) \log(1 - \hat{p}_t(x)) \Big]. \tag{10}$$

In the minimal baseline, $\hat{p}_t$ is derived from a persistence prediction (previous core) with smoothing.

Total misfit, adequacy, and distortion. Total misfit is:

$$S_{\text{total}}(t) = S_{\text{pred}}(t) + \eta S_{\text{coh}}(t), \tag{11}$$

yielding the TRA adequacy proxy $\hat{A}(t) = \exp(-\lambda S_{\text{total}}(t))$ and distortion $\hat{D}(t) = \exp(\lambda S_{\text{total}}(t))$.

5.3 Quantitative predictions and falsifiability

TRA becomes scientific only if it makes quantitative predictions that can fail. The CA testbed enables at least six falsifiable predictions:

P1: Adequacy–identity correlation. For persistence modes, $\hat{A}(t)$ should correlate strongly with identity continuity; non-persistence modes should show weak correlation.

P2: Coherence-cost ordering (matched-budget). Time-averaged coherence cost should satisfy:

$$\langle S_{\text{coh}} \rangle_{\text{active\_persist}} < \langle S_{\text{coh}} \rangle_{\text{active\_random}} \approx \langle S_{\text{coh}} \rangle_{\text{passive\_nopersist}}.$$

Violation falsifies the claim that informational coupling, not action magnitude, reduces coherence cost.

P3: Perturbation distortion spike. A localized shock should increase S_{total} and thus $\hat{D}(t)$; the post/pre distortion ratio should be larger for non-memory modes than for persistence modes.

P4: Intervention budget threshold. There exists β_{crit} below which active_persist is indistinguishable from passive_persist, and above which active_persist dominates.

P5: Cross-mode scaling. Across modes, mean identity should obey:

$$\langle \text{identity} \rangle \approx \exp(-\alpha \langle S_{\text{total}} \rangle),$$

with exponential model selection preferred over linear/power-law alternatives if TRA's form is correct.

P6: Memory-depth saturation. Increasing halo depth improves coherence only up to a saturation scale, beyond which gains vanish.

6 Experimental Design

6.1 Factorial sweep

We sweep boundary mode $\in$ {zero, wrap}, observer mode $\in$ {object_off_tracked, passive_nopersist, passive_persist, a and random seeds ($n = 50$, seeds 0–49). Each run lasts $T = 300$ steps.

6.2 Perturbation protocol

At $t = 150$ we apply a localized stochastic shock: flip cells within radius 10 of the attention center at 3% per cell. Recovery is measured as signed change in core size averaged over $[150, 250]$ relative to baseline $[50, 150]$.

7 Results: Information vs. Energy (The Smoking Gun)

7.1 Identity continuity results

Across seeds and boundary conditions, persistence bias yields high identity continuity with *zero* action, while no-persistence tracking collapses to near-zero continuity. Memory-guided intervention modestly improves continuity further.

7.2 Matched-budget dissociation

The decisive result is the matched-budget control:

active_persist succeeds while active_random fails at the same action rate.

This isolates informational coupling as the causal factor: undirected action (energy without structure) does not sustain continuity.

7.3 Robustness across boundary conditions

The ordering of effects is preserved under toroidal wrap, ruling out dependence on external edges and supporting a relational mechanism intrinsic to the closed system.

7.4 Quantitative summary

Table 1 reports aggregated identity results over $n = 50$ seeds.

Table 1: Identity results across $n = 50$ seeds. Values are mean ± SD. Persistence modes achieve high identity; no-persist and random modes collapse to near-zero.

Boundary	Observer Mode	Mean Identity	n
zero	object_off_tracked	0.646 ± 0.010	50
zero	passive_nopersist	0.0002 ± 0.0003	50
zero	passive_persist	**0.688 ± 0.010**	50
zero	active_persist	**0.700 ± 0.013**	50
zero	active_random	0.0004 ± 0.0003	50
wrap	object_off_tracked	0.610 ± 0.010	50
wrap	passive_nopersist	0.0003 ± 0.0003	50
wrap	passive_persist	**0.675 ± 0.012**	50
wrap	active_persist	**0.694 ± 0.013**	50
wrap	active_random	0.0004 ± 0.0004	50

Table 2 reports explicit misfit metrics computed via the integrated coherence cost calculator.

Table 2: Explicit misfit metrics across $n = 50$ seeds. Mean ± SD per condition.

Boundary	Observer	S_{coh}	S_{pred}	S_{total}
zero	object_off_tracked	5.551 ± 0.020	0.546 ± 0.013	6.097 ± 0.016
zero	passive_nopersist	6.841 ± 0.012	0.002 ± 0.001	6.843 ± 0.012
zero	passive_persist	5.552 ± 0.025	0.059 ± 0.001	5.612 ± 0.024
zero	active_persist	**5.441 ± 0.036**	0.065 ± 0.001	**5.507 ± 0.035**
zero	active_random	6.831 ± 0.013	0.003 ± 0.001	6.835 ± 0.012
wrap	object_off_tracked	5.632 ± 0.018	0.480 ± 0.014	6.112 ± 0.016
wrap	passive_nopersist	6.833 ± 0.013	0.003 ± 0.000	6.836 ± 0.013
wrap	passive_persist	5.552 ± 0.033	0.057 ± 0.001	5.609 ± 0.032
wrap	active_persist	**5.414 ± 0.038**	0.064 ± 0.001	**5.478 ± 0.037**
wrap	active_random	6.825 ± 0.013	0.004 ± 0.001	6.828 ± 0.013

The results confirm prediction P2: $\langle S_{\text{coh}} \rangle_{\text{active}} < \langle S_{\text{coh}} \rangle_{\text{active\_random}}$, demonstrating that informational coupling (not action magnitude) reduces coherence cost.

7.5 Figures

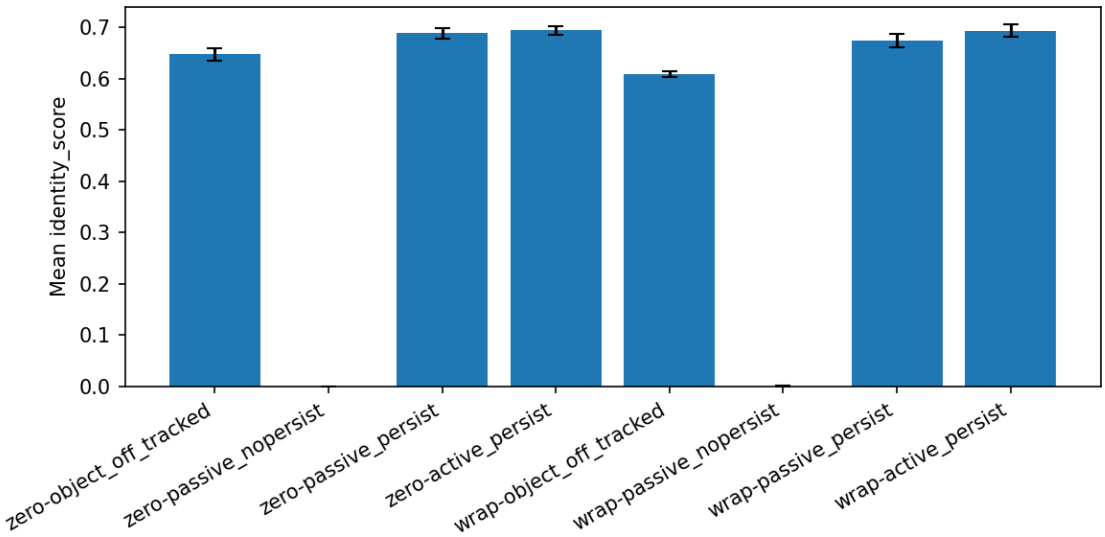

Figure 1: Mean identity score by observer mode and boundary condition.

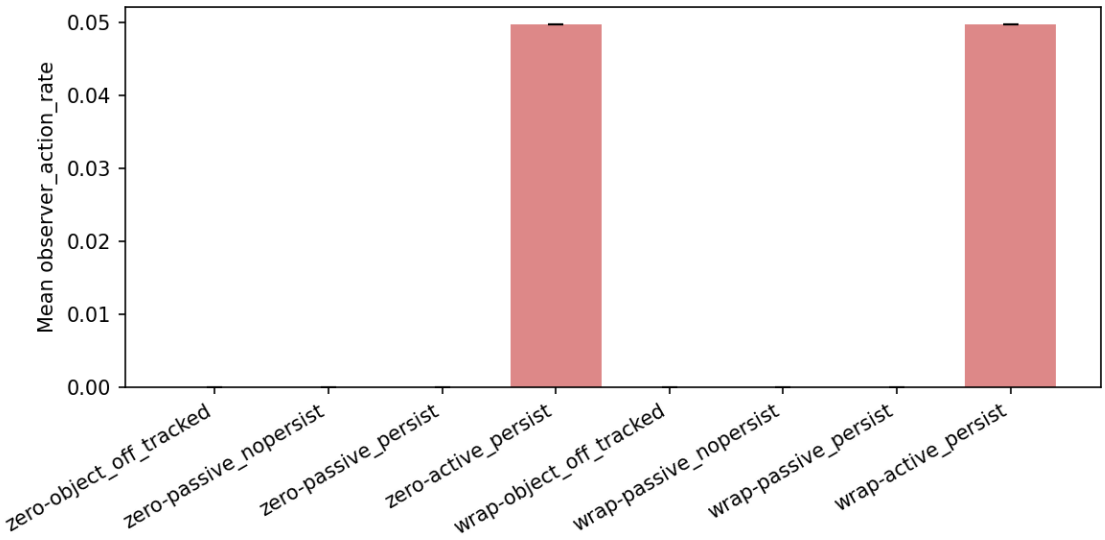

Figure 2: Mean action rate by mode (matched budget in active modes).

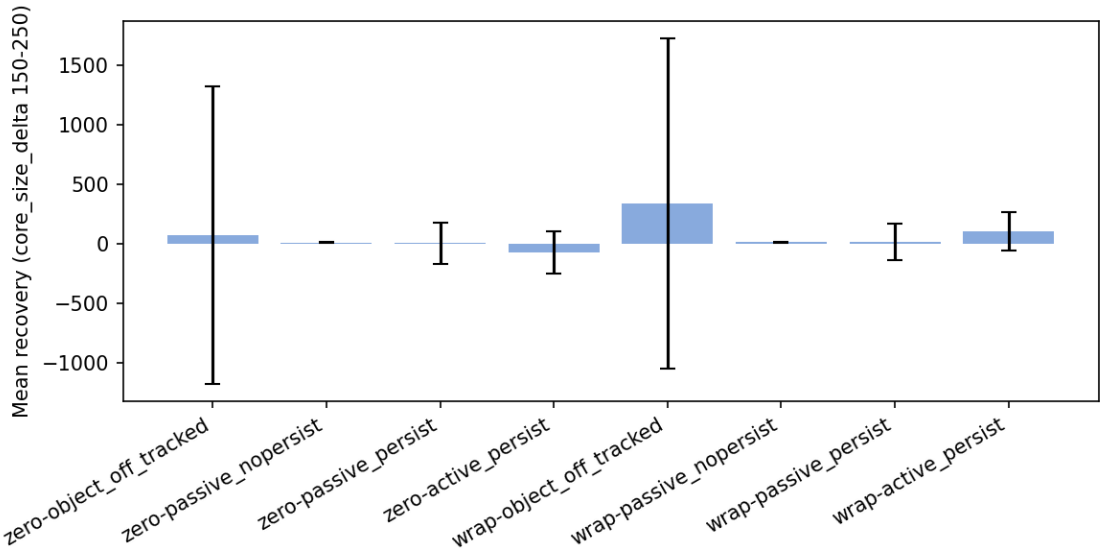

Figure 3: Recovery under perturbation by mode (mean post-shock change relative to baseline).

7.6 Explicit Coherence Cost Results

With explicit S_{coh} computation integrated into the CA loop, we validate the TRA predictions. Figure 4 shows coherence and predictive costs by observer mode: active modes with persistence bias achieve lowest total misfit, while random intervention produces high coherence cost despite matched action budget.

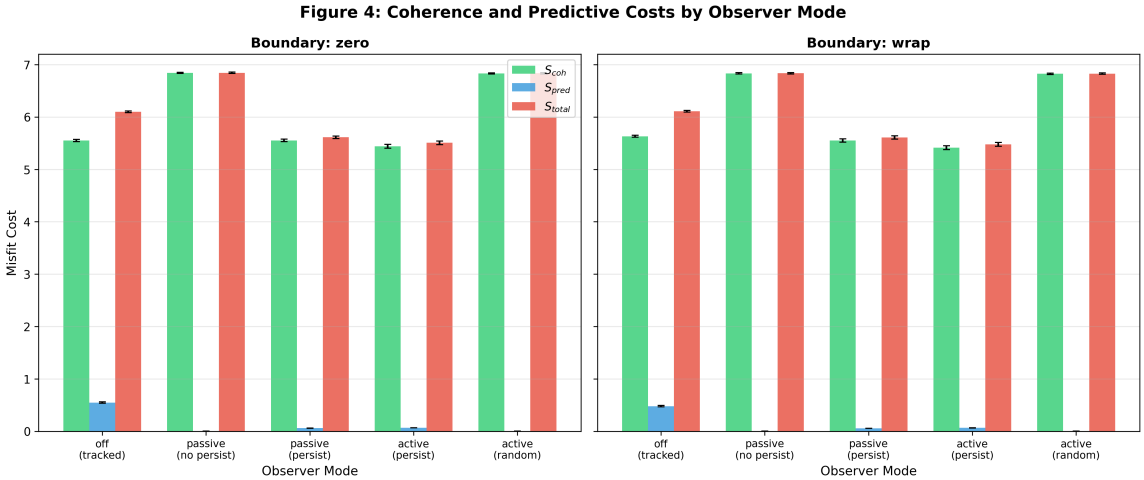

Figure 4: Mean ± SD of coherence cost (S_{coh}), predictive surprisal (S_{pred}), and total misfit (S_{total}) by observer mode. Active persistence achieves lowest total misfit; random intervention yields highest coherence cost despite matched budget.

Figure 5 tests the TRA bridge prediction (P1): adequacy proxy $\hat{A} = \exp(-S_{\text{total}})$ correlates with identity score. Across all modes, the Pearson correlation is $r = 0.887$ (zero boundary, $n = 250$) and $r = 0.892$ (wrap boundary, $n = 250$). Restricting to persistence modes only yields $r = 0.696$ (zero, $n = 100$) and $r = 0.780$ (wrap, $n = 100$), supporting the exponential mapping from misfit to

identity continuity.

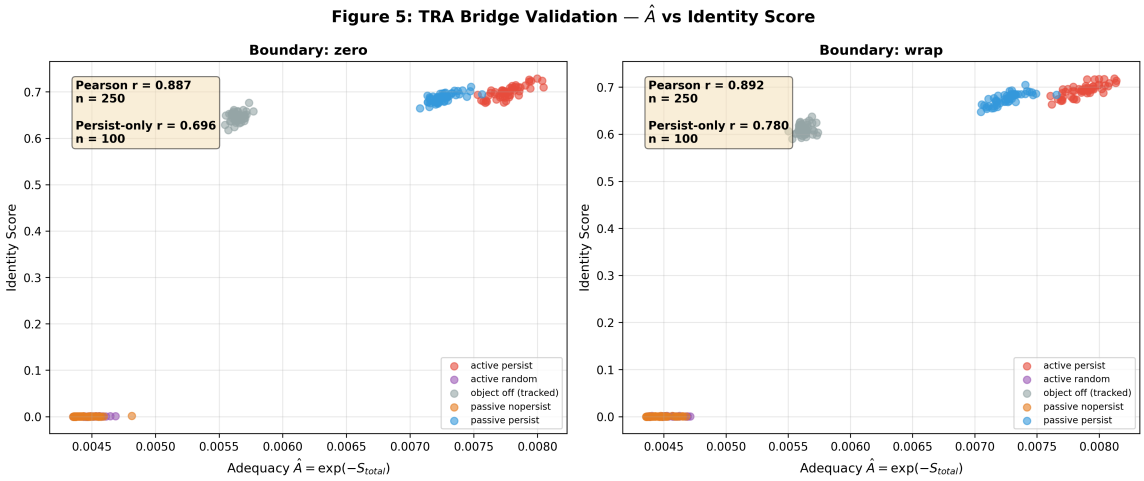

Figure 5: Scatter plot of TRA adequacy proxy $\hat{A} = \exp(-S_{\text{total}})$ versus identity score ($\lambda = 1$). Each point is one run (aggregated over timesteps). For all modes: $r = 0.887$ (zero, $n = 250$), $r = 0.892$ (wrap, $n = 250$). For persistence modes only: $r = 0.696$ (zero, $n = 100$), $r = 0.780$ (wrap, $n = 100$).

8 Discussion

8.1 Informational coupling vs. control magnitude

The matched-budget failure of random intervention blocks a common trivialization: "intervention helps because you forced the system." It does not. Intervention without memory-coupled alignment fails. Therefore the causal variable is not action magnitude but informational coupling to tracked structure.

8.2 What the CA does and does not establish about TRA

Within this paper, "time" is operational: τ is baseline unfolding (simulation step baseline), t is effective alignment duration required by the finite observer-mode to maintain coherence/identity. The CA provides a concrete discriminator for the TRA mechanism, but it does not yet establish a fundamental claim about spacetime; it establishes a falsifiable bridge from misfit to experienced duration in finite computational agents.

8.3 Autopoiesis and boundary-mediated organization

The boundary-driven CA is not a biological model, but it instantiates an operational homology: boundaries shape internal dynamics; memory introduces closure-like constraints; and identity emerges as a maintained relation rather than an intrinsic invariant. This supports a computational approach to studying individuation and organizational continuity.

8.4 Three ontological readings of TRA

TRA admits three increasingly strong interpretations:

1. **Phenomenological:** t describes experienced/computational time for finite observers, leaving τ fundamental.
2. **Effective theory:** for non-equilibrium observers, t is governed by information-thermodynamic constraints emerging from deeper dynamics.
3. **Constitutive:** time is fundamentally relational; τ is an ideal limit as $S_{\text{total}} \to 0$.

This paper supports (1) and provides scaffolding for (2); (3) remains speculative.

8.5 The tautology objection

TRA avoids trivial circularity via (i) the specificity of its functional form (exponential vs. alternatives) and (ii) a matched-budget control that separates action magnitude from informational coupling.

9 Limitations and Future Work

- **Locality:** Replace global distance transform with local approximations to test whether boundary causality survives stricter locality.
- **Parameter sweeps:** β (intervention budget) and halo depth s sweeps test threshold and saturation predictions (P4–P6).
- **Model selection:** Formal AIC/BIC comparison of exponential vs. linear vs. power-law fits for the adequacy–identity relationship.

10 Conclusion

We unify two claims into one testable theory: (i) TRA proposes that experienced time is alignment cost, $t = \tau \exp(\lambda S_{\text{total}})$; (ii) boundary-driven CA experiments show that identity continuity is sustained by informational coupling (memory-guided alignment), not by intervention magnitude. The matched-budget dissociation (active_persist succeeds; active_random fails) is the empirical core connecting ontology to measurement. With explicit S_{coh} computation, the framework becomes quantitatively falsifiable rather than merely philosophical.

Acknowledgments

I thank reviewers for constructive feedback that improved this work. This research received no specific grant from any funding agency in the public, commercial, or not-for-profit sectors.

Data Availability

A reproducibility package (LaTeX sources, exported figures, simulation code, and data) is provided with the supplementary materials for this manuscript.

Conflict of Interest

The author declares no competing interests.

References

[1] J. H. Conway. The game of life. *Scientific American*, 223(4):120–123, 1970.

[2] S. Wolfram. *A New Kind of Science*. Wolfram Media, 2002.

[3] A. Ilachinski. *Cellular Automata: A Discrete Universe*. World Scientific, 2001.

[4] C. G. Langton. Computation at the edge of chaos: phase transitions and emergent computation. *Physica D*, 42(1–3):12–37, 1990.

[5] S. A. Kauffman. *The Origins of Order: Self-Organization and Selection in Evolution*. Oxford University Press, 1993.

[6] H. R. Maturana and F. J. Varela. *Autopoiesis and Cognition: The Realization of the Living*. D. Reidel, 1980.

[7] F. J. Varela. *Principles of Biological Autonomy*. North-Holland, 1979.

[8] F. J. Varela, E. Thompson, and E. Rosch. *The Embodied Mind: Cognitive Science and Human Experience*. MIT Press, 1991.

[9] G. Borgefors. Distance transformations in digital images. *Computer Vision, Graphics, and Image Processing*, 34(3):344–371, 1986.

[10] P. F. Felzenszwalb and D. P. Huttenlocher. Distance transforms of sampled functions. *Theory of Computing*, 8(1):415–428, 2012.

[11] P. Jaccard. Etude comparative de la distribution florale dans une portion des Alpes et du Jura. *Bulletin de la Societe Vaudoise des Sciences Naturelles*, 37:547–579, 1901.

[12] K. Friston. The free-energy principle: a unified brain theory? *Nature Reviews Neuroscience*, 11:127–138, 2010.

[13] R. Landauer. Irreversibility and heat generation in the computing process. *IBM Journal of Research and Development*, 5(3):183–191, 1961.

[14] C. Rovelli. Relational quantum mechanics. *International Journal of Theoretical Physics*, 35:1637–1678, 1996.

[15] W. H. Zurek. Decoherence, einselection, and the quantum origins of the classical. *Reviews of Modern Physics*, 75:715–775, 2003.

[16] A. Clark. Whatever next? predictive brains, situated agents, and the future of cognitive science. *Behavioral and Brain Sciences*, 36(3):181–204, 2013.

[17] S.-i. Amari and H. Nagaoka. *Methods of Information Geometry*. American Mathematical Society, 2000.

[18] M. Csikszentmihalyi. *Flow: The Psychology of Optimal Experience*. Harper & Row, 1990.

[19] J. Hohwy. *The Predictive Mind*. Oxford University Press, 2013.

[20] A. K. Seth and K. J. Friston. Active interoceptive inference and the emotional brain. *Philosophical Transactions of the Royal Society B*, 371(1708):20160007, 2016.

[21] G. Tononi and C. Koch. Consciousness: Here, there and everywhere? *Philosophical Transactions of the Royal Society B*, 370(1668):20140167, 2015.